Electronic Supplementary Material

In-situ thermally rearranged poly(benzoxazole-co-imide) membranes on *α*-alumina substrates for He/CH_4 and He/N_2 separation

Lu Wang[1, 2]*, Zhiqiang Li[1, 5]*, Yangdong He[2], Chenzhi Huang[2], Shijin Chen[3], Xianyun Zhou[4], Xiaosong Fan[4], Wenjing Xie[4], Xuerui Wang[1] (✉)

1 State Key Laboratory of Materials-Oriented Chemical Engineering, College of Chemical Engineering, Nanjing Tech University, Nanjing 211816, China

2 Research Institute of Natural Gas Technology, PetroChina Southwest Oil & Gasfield Company, Chengdu 610299, China

3 PetroChina Southwest Oil & Gasfield Company, Chengdu 610051, China

4 Southern Sichuan Gas District, PetroChina Southwest Oil & Gasfield Company, Sichuan 646000, China

5 Quzhou Membrane Material Innovation Institute, Quzhou 324000, PR China

E-mail: x.wang@njtech.edu.cn

*These authors contributed equally to the work.

1. Supporting Figure

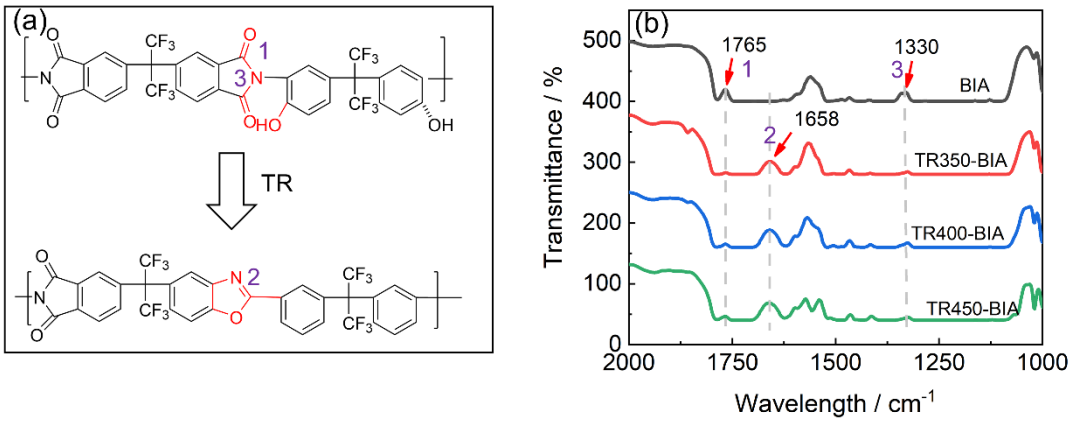

Figure S1 ATR-FTIR spectra of supported 6FDA-APAF-BIA membrane

characterization before and after TR.

The chemical structures of supported 6FDA-APAF-BIA membranes were confirmed by ATR-FTIR (Figure S1). All membranes showed symmetric imide carbonyl absorption bands (C=O, 1) at 1765 cm^{-1} [1]. The bands at 1330 cm^{-1} was transverse stretching and out-of-plane bending of C-N-C groups (3) [2]. The results indicated formation of polyimide structures for all membranes. For TR350-BIA, TR400-BIA and TR450-BIA membranes, a new peak appeared at 1658 cm^{-1} as a C=N (2) telescoping vibration, showing that the generation of benzoxazole rings after thermal rearrangement.

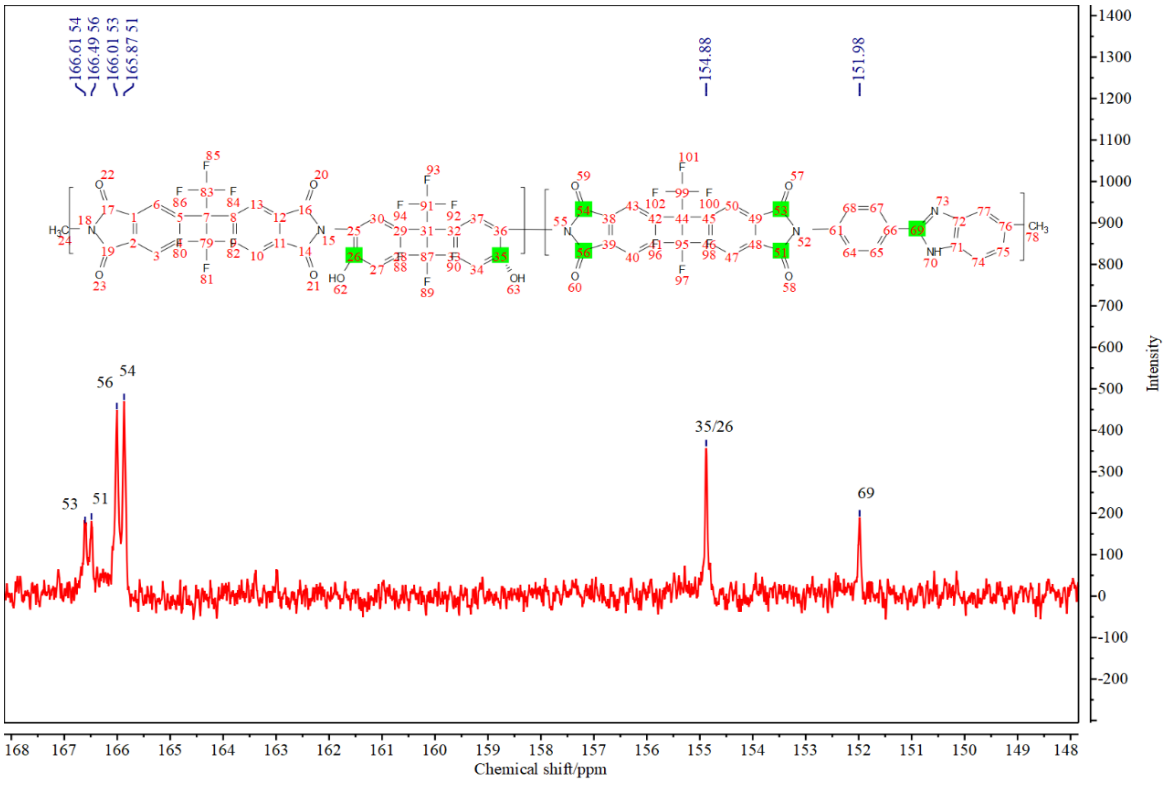

Figure S2 ^{13}C liquid NMR spectroscopy of 6FDA-APAF$_{0.5}$-BIA$_{0.5}$ copolyimide.

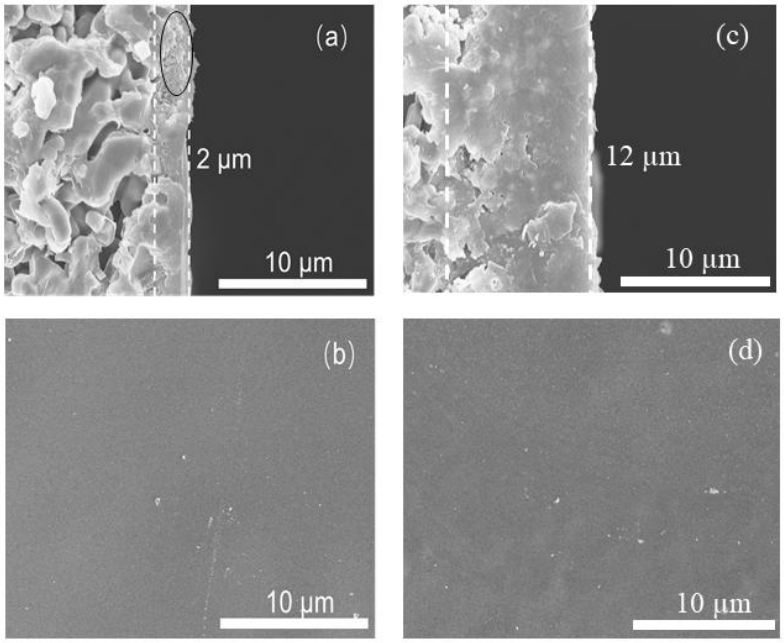

Figure S3 The SEM images of TR450-BIA: (a-b) cross-section and surface of 5 wt.%, (c-d) cross-section and surface of 15 wt.%.

Due to the low viscosity, the solution composed of 5 wt.% polymers lead to defects in the membrane (Figure S3a). On the other hand, the high viscosity of the solution composed of 15 wt.% polymers resulted in a thicker membrane, which would reduce the permeation flux. Therefore, we believe the optimized polymer concentration is 10 wt.% for the coating.

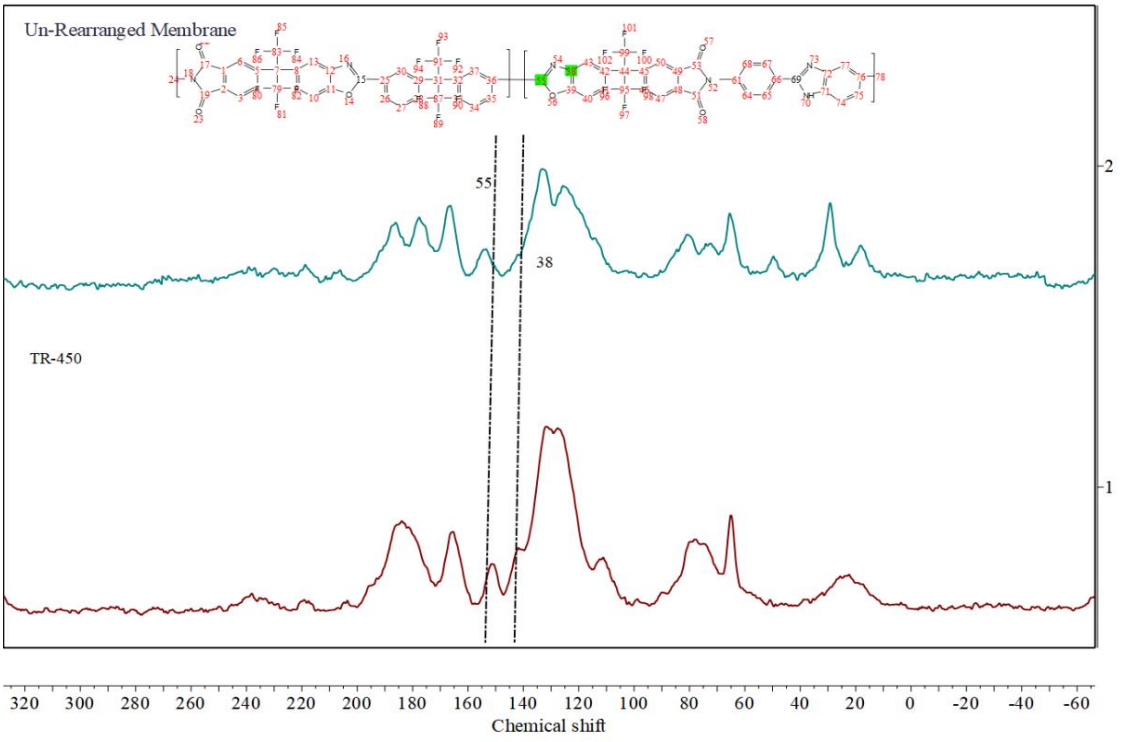

Figure S4 CP/MAS ^{13}C NMR spectroscopy of 6FDA-$APAF_{0.5}$-$BIA_{0.5}$ copolyimide.

The chemical structures of precursor 6FDA-$APAF_{0.5}$-$BIA_{0.5}$ copolyimide also were confirmed by ^{13}C NMR spectroscopy (Figure. S2). Characteristic imide carbonyl signals were observed at around 166 ppm. Specifically, the peaks labeled 53 and 51 correspond to the imide bonds connected to the benzimidazole monomer, while the peaks labeled 54 and 56 indicate the imide bonds not directly connected to the benzimidazole monomer. Additionally, the copolyimide exhibited an additional signal at 151.98 ppm (assigned as peak 69), which is attributed to the C=N bond in the benzimidazole rings. The presence of APAF units within the copolyimide was demonstrated by chemical shifts at 154.88 ppm (peaks labeled 35 or 26). In addition, we have added solid-state ^{13}C CP/MAS NMR to Supporting Information (Figure. S4)

to track the polymer chain rearrangement. As the thermal rearrangement temperature increases to 450 °C, the continuous increase of O-C=N and C-N at 151 ppm (peak labeled 55) and 142 ppm (peak labeled 38) confirms the formation of the benzoxazole ring.

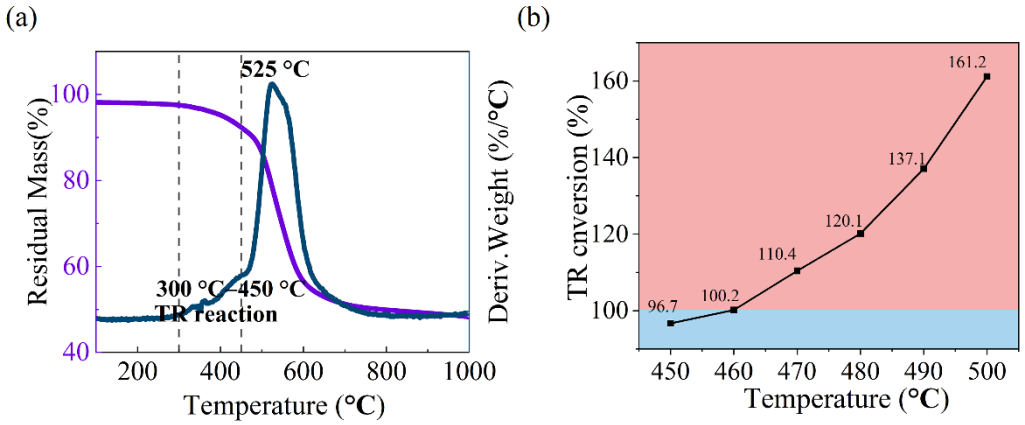

Figure S5 (a) Thermogravimetric analysis (TGA) and derivative thermogravimetry (DTG) curves, showing the thermal rearrangement (TR) reaction peak at 789 K. (b) Thermal conversion rate as a function of temperature (Blue represents thermal transition, and red represents thermal degradation).

A higher temperature is feasible for the TR rearrangement, but the polymer's thermal stability is a critical factor. As shown, the TR ratio exceeds 100% at 460 °C, indicating thermal decomposition. Therefore, a maximum temperature of 450 °C was used in our study, where the TR ratio reached 96.7%. Similarly, Lee *et al*. used 450 °C for the rearrangement of ortho-positioned functional groups [3].

The apparent activation energy of gas permeation ($E_{act,i}$, kJ·mol^{-1}) was determined using the Van't Hoff-Arrhenius equation [4].

$$\ln P_i = a - \frac{E_{act,i}}{R}\frac{1}{T} \quad \text{(S1)}$$

Where P_i is the permeance of component i, GPU; T represents for absolute temperature, K; R is ideal gas constant, 8.314 $J \cdot mol^{-1} \cdot K^{-1}$.

The apparent energies of gas permeation in supported TR450-BIA membrane were defined according to Henry regime [5]:

$$E_{act} = E_{diff} + Q_{St} \quad \text{(S2)}$$

Where E_{diff} (positive) is diffusivity activation energy, $kJ \cdot mol^{-1}$; Q_{St} (negative) is adsorption enthalpy. Due to non-adsorptive nature of He [6], its adsorption enthalpy is considered negligible. Consequently, the diffusion activation energy can be considered equivalent to the apparent activation energy.

2. Supporting Tables

Table S1 Molecular weight data co-polyimide precursors.

	Mn / 10^4 g·mol^{-1}	Mw / 10^4 g·mol^{-1}	PDI / M_w/M_n
6FDA-APAF-BIA	1.3182	3.0880	2.34

Table S2 He/CH_4 and He/N_2 separation performance of supported TR450-BIA membrane comparison with the state-of-the-art membranes.

Membranes	He/CH_4 system			He/N_2 system			Ref
	P_{He} / GPU	S_{He/CH_4} / -	α_{He/CH_4} / -	P_{He} / GPU	S_{He/N_2} / -	α_{He/N_2} / -	
TR-6FDA-APAF	2.4	37.2	N.A.	2.4	26.4	N.A.	[7]
TR-6FDA-APAF-BOA	2.6	85.6	N.A.	2.6	46.7	N.A.	[8]

TR-6FDA-APAF-BIA	2.2	139.8	N.A.	2.2	72.2	N.A.	[8]
TR-6FDA-APAF-DAM	4.9	29.3	N.A.	4.9	19.3	N.A.	[9]
TR-6FDA-APAF-ODA	1.9	81.0	N.A.	1.9	43.1	N.A.	[9]
TR-6FDA-APAF-ADHAB	5.1	28.0	N.A.	5.1	19.3	N.A.	[10]
TR-6FDA-APAF-Cardo	14.1	64	66.4	13.7	52	54.4	[11]
Cellulose acetate	28.0	40.0	N.A.	28.0	46.7	N.A.	[12]
Nafion -117	32.0	56.3	N.A.	32.0	94	N.A.	[13]
Poly (PFMD)	7.0	1650.0	N.A.	7.0	295.8	N.A.	[14]
Poly (PFMMD)	11.2	280.0	N.A.	11.2	72.7	N.A.	[14]
PIM-EA-TB	14.2	3.7	N.A.	14.2	4.90	N.A.	[15]
PIM-SBI-TB	5.6	2.0	N.A.	5.6	3.8	N.A.	[15]
Fluorinated PIM	202	61.2	N.A.	202	36.1	N.A.	[16]
FPIM-5	16.6	3770	N.A.	16.6	857	N.A.	[17]
Poly(*o*-acyloxyamide)s	0.5	106.0	N.A.	0.5	84.0	N.A.	[18]
PSF	0.52	49.0	N.A.	0.52	52.0	N.A.	[19]
STT	37.1	87.0	63.5	35.4	20.0	11.7	[20]
SAPO-34	554.1	N.A.	13.8	N.A.	N.A.	N.A.	[21]
DD3R	13.6	79.0	59.0	13.6	2.9	N.A.	[22]
6FDA-APAF$_{0.5}$-Cardo$_{0.5}$/Al_2O_3	12.5	N.A.	78.8	12.1	N.A.	55.0	[11]
TR-6FDA-APAF$_{0.5}$-Cardo$_{0.5}$/Al_2O_3	40.0	71.2	74.3	40.0	60.0	50.0	[11]
Supported TR450-BIA-1	25.3	123	120	25.3	85	82	
Supported TR450-BIA-2	26.2	125	121	26.2	87	84	This
Supported TR450-BIA-3	24.5	127	120	24.5	89	85	work
Supported TR450-BIA-4	23.8	122	119	23.8	84	81	

87

Table S3 The fitting parameters and apparent permeation activation energy of supported TR450-BIA for He/N_2 and He/CH_4 binary mixture.

		Linear fitting parameters		E_{act}	E_{diff}
		Intercept (a)	Slope ($-\frac{E_{act,i}}{R}$)	kJ·mol^{-1}	kJ·mol^{-1}
He/N_2	He	-6.97	-1.13	9.4	9.4
	N_2	-4.38	-1.70	14.1	-
He/CH_4	He	-7.02	-1.14	9.5	9.5
	CH_4	-4.47	-1.84	15.3	-

3. Supporting References

1. Zhuang Y, Seong J G, Do Y S, Jo H J, Lee M J, Wang G, Guiver M D, Lee Y M. Effect of iomerism on molecular packing and gas transport properties of poly(benzoxazole-co-imide)s. Macromolecules, 2014, 47: 7947-7957

2. Comesaña-Gándara B, Calle M, Jo H J, Hernández A, de la Campa J G, de Abajo J, Lozano A E, Lee Y M. Thermally rearranged polybenzoxazoles membranes with biphenyl moieties: Monomer isomeric effect. Journal Of Membrane Science, 2014, 450: 369-379

3. Park H B, Jung C H, Lee Y M, Hill A J, Pas S J, Mudie S T, Van Wagner E, Freeman B D, Cookson D J. Polymers with cavities tuned for fast selective transport of small molecules and ions. Science, 318 (2007) 254-258.

4. Wang X, Shan M, Liu X, Wang M, Doherty C M, Osadchii D, Kapteijn F. High-performance polybenzimidazole membranes for helium extraction from natural gas. ACS Applied Materials & Interfaces, 2019, 11: 20098-20103

5. Shan M, Liu X, Wang X, Yarulina I, Seoane B, Kapteijn F, Gascon J. Facile manufacture of porous organic framework membranes for precombustion CO_2 capture. Science Advances, 2018, 4(9): eaau1698

6. Gumma S, Talu O. Gibbs dividing surface and helium adsorption. Adsorption, 2003, 9: 17-28

7. Calle M, Lee Y M. Thermally rearranged (TR) poly(ether−benzoxazole) membranes for gas separation. Macromolecules, 2011, 44: 1156-1165

8. Zhuang Y, Seong J G, Lee W H, Do Y S, Lee M J, Wang G, Guiver M D, Lee Y M. Mechanically tough, thermally rearranged (TR) random/block poly(benzoxazole-co-imide) gas separation membranes. Macromolecules, 2015, 48: 5286-5299

9. Jo H J, Soo C Y, Dong G, Do Y S, Wang H H, Lee M J, Quay J R, Murphy M K, Lee Y M. Thermally rearranged poly(benzoxazole-co-imide) membranes with superior mechanical strength for gas separation obtained by tuning chain rigidity. Macromolecules, 2015, 48: 2194-2202

10. Aguilar-Lugo C, Álvarez C, Lee Y M, de la Campa J G, Lozano Á E. Thermally rearranged polybenzoxazoles containing bulky adamantyl groups from ortho-substituted precursor copolyimides. Macromolecules, 2018, 51: 1605-1619

11. Wang L, Li Y, Zhang P, Chen X, Nian P, Wei Y, Lu H, Gu X, Wang X. Thermally rearranged poly(benzoxazole-co-imide) composite membranes on α-Al_2O_3 support for helium extraction from natural gas. Journal of Membrane Science, 2022, 657: 120614

12. Gantzel P K, Merten U. Gas separations with high-flux cellulose acetate membranes. Industrial & Engineering Chemistry Process Design & Development, 1970, 9: 331-332

13. Choi S H, Qahtani M S, Qasem E A. Multilayer thin-film composite membranes for helium enrichment. Journal of Membrane Science, 2018, 553: 180-188

14. Yavari M, Fang M, Nguyen H, Merkel T C, Lin H, Okamoto Y. Dioxolane-based perfluoropolymers with superior membrane gas separation properties. Macromolecules, 2018, 51: 2489-2497

15. Carta M, Malpass-Evans R, Croad M, Rogan Y, Jansen J C, Bernardo P, Bazzarelli F, McKeown N B. An efficient polymer molecular sieve for membrane gas separations. Science, 2013, 339: 303-307

16. Seong J G, Lee W H, Lee J, Lee S Y, Do Y S, Bae J Y, Moon S J, Park C H, Jo H J, Kim J S, Lee K R, Hung W S, Lai J Y, Ren Y, Roos C J, Lively R P, Lee Y M. Microporous polymers with cascaded cavities for controlled transport of small gas molecules. Science Advances, 2021, 7: eabi9062

17. Ma X, Li K, Zhu Z, Dong H, Lv J, Wang Y, Pinnau I, Li J, Chen B, Han Y. High-

performance polymer molecular sieve membranes prepared by direct fluorination for efficient helium enrichment. Journal of Materials Chemistry A, 2021, 9: 18313-18322
18. Díez B, Cuadrado P, Marcos-Fernández Á, Prádanos P, Tena A, Palacio L, Lozano Á E, Hernández A. Helium recovery by membrane gas separation using poly(o-acyloxyamide)s. Industrial & Engineering Chemistry Research, 2014, 53: 12809-12818
19. McHattie J S, Koros W J, Paul D R. Gas transport properties of polysulphones: 2. Effect of bisphenol connector groups. Polymer, 1991, 32(14): 2618-2625
20. Gong C, Peng X, Zhu M, Zhou T, You L, Ren S, Wang X, Gu X. Synthesis and performance of STT zeolite membranes for He/N_2 and He/CH_4 separation. Separation and Purification Technology, 2022, 301: 121927
21. Denning S, Lucero J, Koh C A, Carreon M A. Chabazite zeolite SAPO-34 membranes for He/CH_4 separation. ACS Macro Letters, 2019, 1: 655-659
22. Zhang P, Gong C, Zhou T, Du P, Song J, Shi M, Wang X, Gu X. Helium extraction from natural gas using DD3R zeolite membranes. Chinese Journal of Chemical Engineering, 2021, 49: 122-129